Orientation of Montmorillonite Clay in Dicyclopentadiene/Organically Modified Clay Dispersions and Nanocomposites

Mitra Yoonessi,[1] Hossein Toghiani,[2] Charles U. Pittman Jr.[3]

[1]*Wright Patterson Air Force Research Laboratory, WPAFB, Ohio 45433*
[2]*Dave C. Swalm School of Chemical Engineering, Mississippi State University, Mississippi 39762*
[3]*Department of Chemistry, Mississippi State University, Mississippi 39762*

Received 30 November 2005; accepted 24 January 2006
DOI 10.1002/app.24387
Published online in Wiley InterScience (www.interscience.wiley.com).

ABSTRACT: Highly delaminated dispersions of the organically modified clay I-28 (Nanocor, Inc.) in liquid dicyclopentadiene (DCPD) were prepared. *In situ* ring-opening metathesis polymerization of I-28/DCPD nanodispersions generated I-28/poly(DCPD) nanocomposites. When clay/DCPD dispersions were cured under shear, alignment of clay platelets, tactoids, and small particles was captured. This orientation was confirmed by X-ray diffraction and transmission electron microscopy. The Herman's orientation parameters were calculated for the oriented nanocomposites. Viscosities of these liquid nanodispersions exhibited thixotropic flow behavior, prior to curing. The time-dependent viscosity effects became more pronounced with an increase in delamination. Initial viscosities increased with progressive clay platelet generation during delamination and nanodispersion within the liquid monomer. Viscosity can be used to follow clay exfoliation/delamination. Etching the surface of a 2 wt % I-28 clay/poly(DCPD) nanocomposite with oxygen plasma eroded the matrix, exposing clay tactoids protruding from the surface. These surfaces were examined by SEM and energy dispersive X-ray spectroscopy. J Appl Polym Sci 102: 2743–2751, 2006

Key words: nanoclay; nanocomposites; SAXS; viscosity

INTRODUCTION

Rheological studies of nanodispersions are becoming more significant with an increase in the applications of nanophases in engineering materials. The thixotropic behavior of the clay particles in water suspensions, including yield stress measurements and shear thinning behavior, has been well studied in water.[1–7] In montmorillonite/water dispersions, clay particle aggregation can occur with temperature changes. Electrolytes strongly affect the flow behavior of such suspensions.[3,8] Clay suspensions also produce gel-like structures, and their deformations under applied stresses have an elastic component.[2,5] The timescale of these measurements are important, since clay suspensions are viscoelastic fluids.[2,4,5,9]

Montmorillonite clay consists of stacks of 1-nm thick alumina silicate sheets called platelets. Each platelet is made of an alumina octahedral sheet sandwiched between two silica tetrahedral sheets. Owing to the attractive force between the clay platelets, commonly, clay dispersion results in the formation of platelet stacks called tactoids. Montmorillonite clays are the most widely employed dispersed clay phases for nanodispersions and nanocomposites.[1–17] Their nanocomposites have shown superior mechanical properties, gas permeability resistance, and flame resistance.[10–17] The viscosity behavior of organically modified montmorillonite clay/monomer nanodispersions is particularly important during processing, before monomer polymerization or resin curing. Rheological properties are critical during the compounding/processing of layered silicates in polymer melts (melt intercalation or exfoliation). Rheology is also a major variable when infusing nanoparticle/resin formulations into fiber preforms and between the fibrils of fiber tows in VARTM and related processes.[18]

In this article, we report the viscosity changes of alkyl ammonium ion-modified montmorillonite clay/dicyclopentadiene dispersions, with the extent of clay exfoliation and the orientation of the intercalated/partially delaminated clay under the shear.

Dicyclopentadiene (DCPD) is a low viscosity monomer that can be polymerized into highly crosslinked polymer networks.[19–23] *In situ* polymerization has already been used as an efficient method to incorporate nanodispersed clay into poly(DCPD) (PDCPD).[23]

Correspondence to: M. Yoonessi (mitra.yoonessi@wpafb.af.mil).

Contract grant sponsor: The Air Force Office of Scientific Research; contract grant number: F49620-02-1-026-0.

Contract grant sponsor: National Science Foundation; contract grant number: EPS0132618.

Highly delaminated, organically modified montmorillonite/polyDCPD composites with random tactoid orientation have been prepared and examined by a variety of methods (XRD, SAXS, TEM, SANS, and HR-TEM) and reported in detail.[23,24]

The state of clay dispersion in a solvent or monomer is critically important during the delamination process, before *in situ* polymerization of the monomer or mixing into an existing polymer. When clay is dispersed as a mixture of single clay platelets and tactoids within the monomer and the polymer matrices, it is called highly delaminated dispersion and nanocomposite. Exfoliated clay platelet dispersions and nanocomposites are dispersion of single clay platelet within the monomer or polymer. Tactoids are stack of clay platelets that are significantly smaller than a clay particle, but consist of two or more platelets. If a highly exfoliated nanodispersed state can be achieved in a liquid monomer, subsequent polymerization of that monomer could lead to a composite with a highly dispersed clay platelets. A correlation between the increase in viscosity and the degree of clay delamination is reported herein. Viscosity can be used as an online measurement criteria to estimate the degree of clay delamination before carrying out the polymerization step. Alignment of clay tactoids and exfoliated platelets in the DCPD under shear was captured by *in situ* polymerization of this monomer via ring-opening metathesis polymerization (ROMP).

EXPERIMENTAL

Materials and preparations

Nanomer® I-28 was provided by Nanocor and used as received. I-28 is a montmorillonite clay, which has been ion-exchanged with the trimethyldodecadecyl alkylammonium ion. This clay has a *d*-spacing of 2.25 nm. Dicyclopentadiene (DCPD) was provided by Cymetech, LLC under the trade name of Ultrene™99 (99.2% pure). A first generation Grubbs' metathesis catalyst, dichloro(3-methyl-2-butenylidene)-bistricyclopentylphosphine ruthenium, was used to cure the I-28 clay/DCPD dispersions. Ethylene glycol monoethyl ether (EGME, 2-ethoxyethanol) 99% was provided from Aldrich.

Clay I-28 was dispersed in liquid DCPD by stirring for 1 h, followed by sonication for 3 h under nitrogen. Sonication was performed at 20 kHz, with a wave amplitude of 30, using a 500 W sonication model GE501 ultrasonic processor (Ace Glass). The concentration range of clay employed in this study was 0.005–5 wt %. Cyclopentadiene (4 wt %) was used as a comonomer to reduce the melting point of DCPD from 39°C to below room temperature. The *d*-spacing of clay layers within the liquid DCPD was followed by X-ray diffraction (XRD), after curing each sample, and these values were reported elsewhere.[23,24] The viscosities of low clay concentration dispersions were measured in Cannon-Ubbelhode viscometers. A Couette flow corotating cylinder viscometer was used to examine the viscosities of these suspensions as a function of clay nanodispersion in DCPD and as a function of clay loading levels.

The clay/DCPD dispersions were sonicated to achieve delaminated and intercalated clay monomer dispersions. Then the dispersions were placed in a corotating cylinder geometry, and shear was applied to the dispersion. Polymerization was carried out by adding sufficient amounts of the fist generation Grubbs catalyst to the 2 and 5 wt % I-28 clay/DCPD dispersions, while shearing. At the same time, the temperature was increased to facilitate fast curing and thereby capture the clay alignment by rapid *in situ* ring-opening metathesis polymerization (ROMP). This facilitated fast curing of the clay/monomer dispersion and thereby captured the clay alignment under the shear.

The specific surface area (SSA) of clay I-28 was determined experimentally using the EGME method described by Cerato and Lutengger, and Eirich [25,26] This method assumes that a monolayer of EGME is adsorbed to the clay surface.[25] EGME (3 mL) is added to the clay (1 g) and stirred. The suspension is placed in a vacuum oven for 24 h, until unadsorbed EGME is removed. Then, the SSA of clay is calculated from SSA $= W_a/0.000286W_s$, where SSA is the specific surface area, W_a is the adsorbed EGME and W_s is the original weight of clay.

Characterization

Viscometry measurements

A Brookfield concentric cylinder viscometer, model DV-I, with LV spindles was used. Viscometry measurements were performed at 29°C in a Couette flow concentric cylinder geometry. The outer cylinder was stationary and the inner cylinder (spindle) was rotating. The torque signal was transformed to shear stress, and the data were collected using Camile 2200® control software to monitor the process. Then, the signal was processed and transformed into a viscosity value using CamileTG® software.

Shear rate and shear stress in a corotating cylinder are calculated from the following equations:

$$S = \frac{2\omega R_c^2 R_b^2}{x^2(R_c^2 - R_b^2)} \quad (1)$$

$$F' = \frac{T}{2\pi R_b^2 L} \quad (2)$$

where S is shear rate, ω is angular velocity, R_b and R_c are inner and outer cylinder radii, x is distance, F'

is shear stress, T is the torque, and L is the cylinder length. Viscosity is the ratio of the shear stress to shear rate.

XRD measurements

XRD analysis was used to follow the clay's d-spacing in the cured nanocomposites versus the extent of mixing and sonication used during dispersion. XRD data for the starting clay powder and for the clay/P(DCPD) nanocomposites were collected on a Philips diffractometer, model X'Pert, using Cu Kα radiation ($\lambda = 0.154056$ nm). Scans were taken over the 2θ range of 1–10°, with a step size of 0.03° at 1 s per step.

Wide angle XRD

The X-ray scattering regime was collected using an evacuated Statton camera (Warhus, DE) with a point-collimated X-ray beam via two pinholes (0.05 mm), separated by ~15 cm at Cu Kα wavelength of 1.5418 Å.

Transmission electron microscopy

A JEM-100CX II transmission electron microscope (TEM, 60 kV) was used to examine clay morphology and orientation. Nanocomposite samples were ultramicrotomed to thicknesses of 70–85 nm at room temperature, using a Reichert-Jung Ultracut E ultramicrotome equipped with a diamond knife. The samples were placed on a Formvar-coated 200-mesh copper grid. The clay versus polymer matrix contrast was sufficient to permit electron micrograph imaging without staining.

Scanning electron microscopy

A Leo Stereoscan 360 scanning electron microscope, 40 kV, with a resolution of 25 Å and containing a tungsten filament was used to examine the surface of the clay/polyDCPD composites. This instrument was equipped with an energy dispersive X-ray spectrometer (EDS) and a Princeton Gamma-Tech eXcalibur software for electron beam-induced energy dispersive X-ray analysis.

The composite surfaces were coated with Au/Pd by sputter coating using a Polaron E5100 sputter coater, to produce a Au/Pd coating with a nominal thickness of 40–50 nm on the surface of the composites. Target to specimen distance was 50 mm. Sputter coating was performed in an ionized argon gas at low pressure using a 2.5 kV voltage.

Oxygen plasma

Oxygen plasma treatments were performed using a Technics PEII-A plasma generator, using radio frequency (RF) under a 30–35 mTorr vacuum and 100 W power. Samples were treated for 30 and 60 s.

RESULTS AND DISCUSSION

Stirring clay I-28 into DCPD caused expansion of clay layers from a d-spacing of 2.25–4.15 nm.[23] This expansion is the result of nonpolar DCPD intercalating into the clay galleries, which have been pillared by the long dodecadecyl hydrocarbon chain of the exchanged ammonium ions. The separation of clay particles in the suspension to a highly delaminated mixture of clay platelets and tactoids was achieved after 3 h of sonication [Fig. 1(a)].[23,24] The progressive loss of the 4.15 nm d-spacing XRD peak as sonication proceeds [Fig. 1(a)] tracks this advance of delamina-

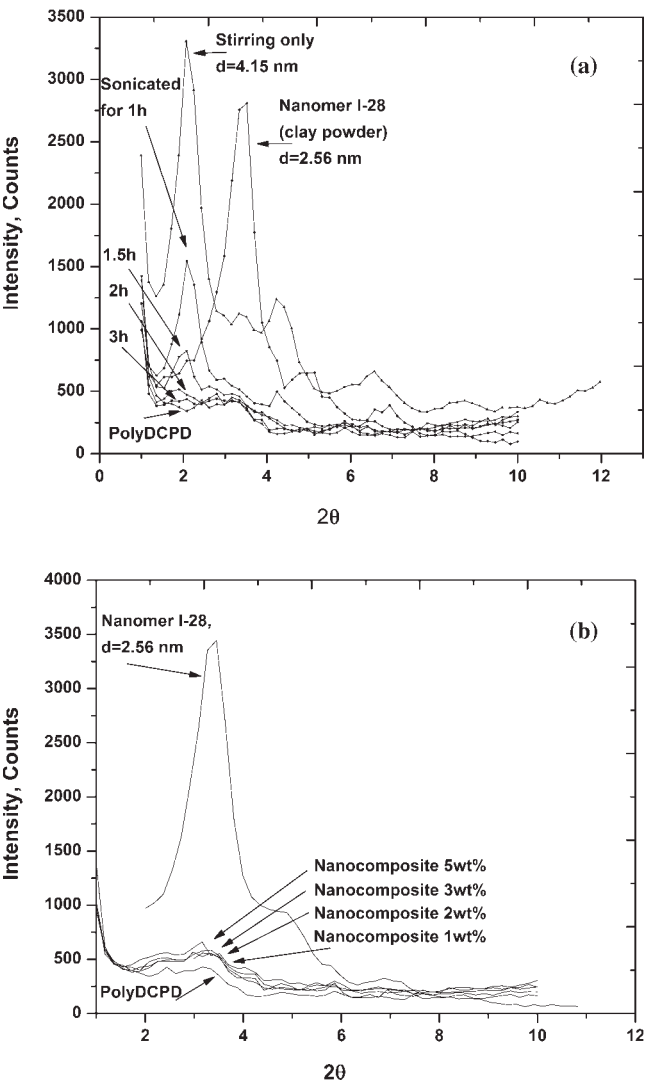

Figure 1 PolyDCPD composites delaminated by stirring and sonication. (a) XRD plots of 0.5 wt % I-28 in DCPD liquid versus sonication time compared to polyDCPD and the initial clay powder. (b) XRD plots of 1–5 wt % I-28 clay/composites sonicated for 3 h.

tion in nanodispersion. The polyDCPD 1–5 wt % I-28 clay nanocomposites were then prepared by ROMP of these DCPD/I-28 liquid nanodispersions. The I-28 clay's XRD peak in these nanocomposites was absent, just as it was in their liquid nanodispersion precursors [Fig. 1(b)]. Extensive X-ray and neutron scattering studies, already reported, verified the existence of a highly delaminated clay nanocomposite after a 3-h sonication treatment of clay I-28 in DCPD monomer prior to curing.[24] Figure 2(a) shows a clay particle, some tactoids, and a few exfoliated platelets after a 1-h sonication of 0.5 wt % clay I-28 in DCPD followed by curing. Clay platelets and tactoids are being splayed apart from the original particle. Another aliquot of this same dispersion was subjected to longer sonication (3 h) and then polymerized. TEM micrographs [Fig. 2(b)] confirmed the existence of a highly delaminated nanocomposite containing dispersed individual platelets, and small tactoids had formed after 3 h of sonication.

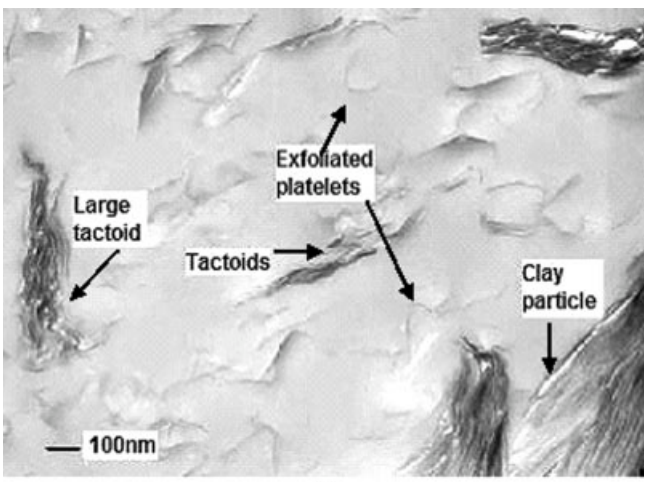

(a)

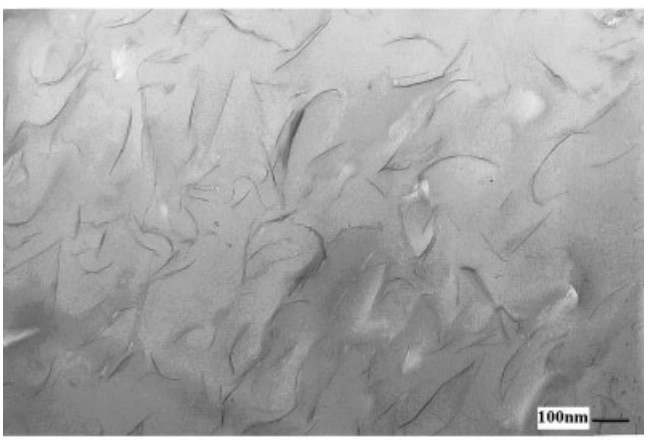

(b)

Figure 2 Delamination of clay I-28 in polyDCPD (0.5 wt %) composites versus sonication time. (a) Partial delamination of clay (1-h sonication). (b) Highly delaminated clay I-28/polyDCPD composite (3-h sonication).

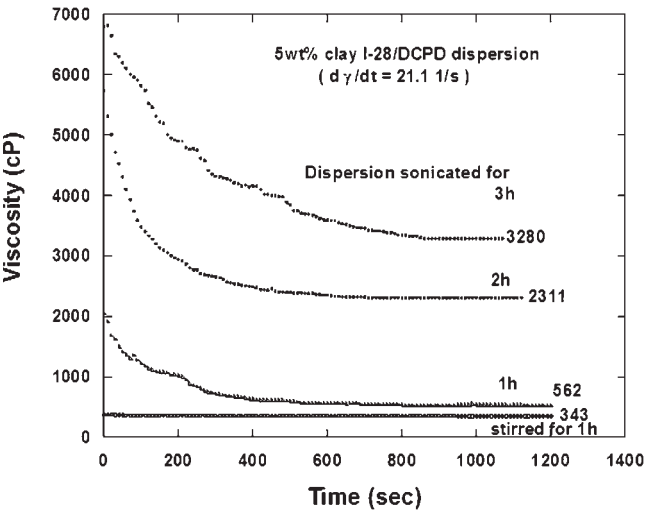

Figure 3 Viscosity of 5 wt % clay I-28/DCPD dispersions. The viscosities were measured both as a function of time and the degree of delamination at constant shear rate (21.09 s^{-1}).

Viscometry

The viscosity of the I-28 clay/DCPD dispersions was studied as a function of clay delamination. A Cannon-Ubbelhode viscometer was used to examine low clay concentrations (0.005–0.5 wt %). Only suspensions at the highest degree of delamination (after 3 h of sonication) were studied. The relative viscosities, η_{rel}, were determined from the viscosity of the dispersion, η', and the viscosity of liquid DCPD, η, ($\eta_{rel} = \eta'/\eta$). The relative viscosities were 1.15, 1.16, and 1.28 for the 0.05, 0.08, and 0.14 wt % I-28/DCPD dispersions, respectively. These viscosities did not exhibit a time-dependent behavior. However, changes of viscosity with the measurement time were observed at a clay concentration of 0.5 wt % and higher. The clay is present as well-dispersed tactoids and platelets in the very low concentration suspensions (0.005–0.5 wt %). The increased clay surface area due to delamination is not yet large enough to induce detectable time-dependent behavior, because the concentration is very low.

The viscosity measurements of clay suspension concentrations above 0.5 wt % were followed using the corotating cylinder viscometer. Increasing clay concentrations resulted in a time-dependent viscosity behavior. The 5 wt % I-28/DCPD suspension exhibited viscosities that are dependent on both the time of shearing and clay loadings (Fig. 3). The viscosity decreased with shearing time, indicating a thixotropic behavior of this suspension. The initial viscosities (at the start of shearing) increased, as more clay nanolayers, small tactoids, and platelets, were formed (extended sonication time).

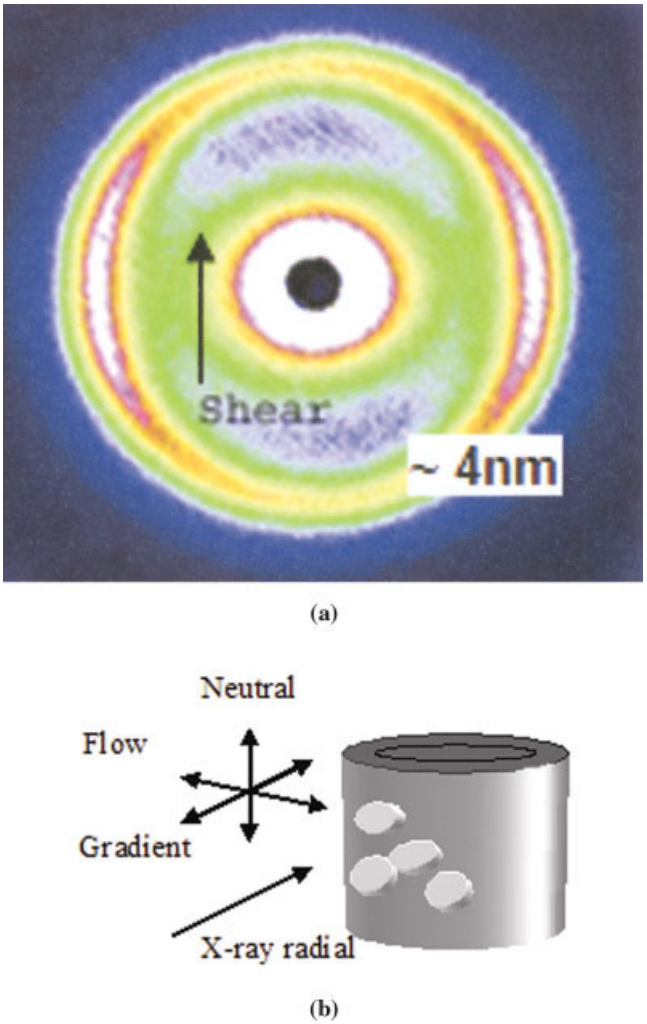

Figure 4 Two-dimensional X-ray scattering of the partially delaminated 5 wt % I-28/DCPD composite cured under shear. (a) 2D scattering of partially delaminated clay composite. (b) The direction of the incident X-ray beam respect to the flow is radial. Data were collected after curing the nanocomposite (*ex situ*). [Color figure can be viewed in the online issue, which is available at www.interscience.wiley.com.]

The differences between initial and steady state viscosities also become larger as clay delamination proceeded at constant clay concentration. Increased thixotropic flow behavior was observed with increased delamination of clay nanolayers when holding the clay loading level constant at 5 wt %, (Fig. 3). More resistance to flow occurs with more platelets present, resulting in a stronger thixotropic behavior. At constant clay concentration, viscosity increases are caused by the generation of more surface area as the delamination proceeds. The difference between the initial and steady state viscosities becomes larger, as larger number of randomly oriented clay nanophases are generated during sonication. More platelets cause more resistance to flow. Viscosity drops rapidly from its initial value as shearing continues, because the nanolayers tend to align themselves in the direction of flow.

After 3 h of sonication, the initial viscosity of the dispersion did not further increase with continued sonication. This indicates that no further significant nanodispersion/exfoliation was occurring. This was observed even for the 5 wt % clay I-28/DCPD dispersion after 3 h of sonication.

Viscosity measurements provide a means to follow the progress of nanodispersion in the lab or as a process control method. Accurate viscosity measurements versus the state of clay delamination can serve as a criteria for evaluating the degree of clay dispersion/delamination. Furthermore, viscosity measurements are a tool to determine whether or not highly delaminated dispersions are achieved.

X-ray diffraction

The partially delaminated 5 wt %I-28/DCPD composite (1 h sonication), cured under shear, was examined by XRD (Fig. 4).The scattering from this composite shows a peak at $\sim$ 4 nm as evidence of intercalation and partial delamination. The presence of distinct arcs in 2-D X-ray scattering data is a clear indication of alignment of clay platelets and tactoids under shear. This is diffraction from intercalated layers, and scattering from clay particles will appear in the small angle regime. The degree of orientation can be calculated from azimuthal width of the arcs.[27,28] Figure 5 shows the azimuthally averaged scattering intensity versus the scattering angle after corrections and background subtraction. The orientation parameter was calculated according to eq. (3), assuming a cylindrical geometry of clay tactoids.[28]

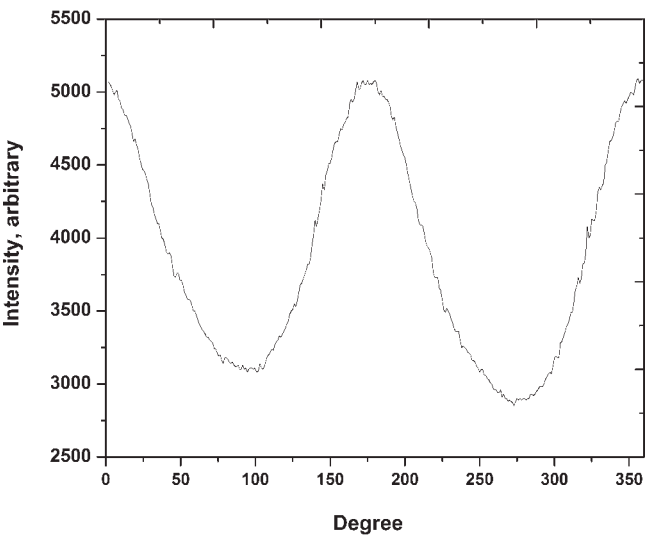

Figure 5 Azimuthally averaged intensity of scattering versus scattering angle of the 5 wt % I-28/DCPD composite sample.

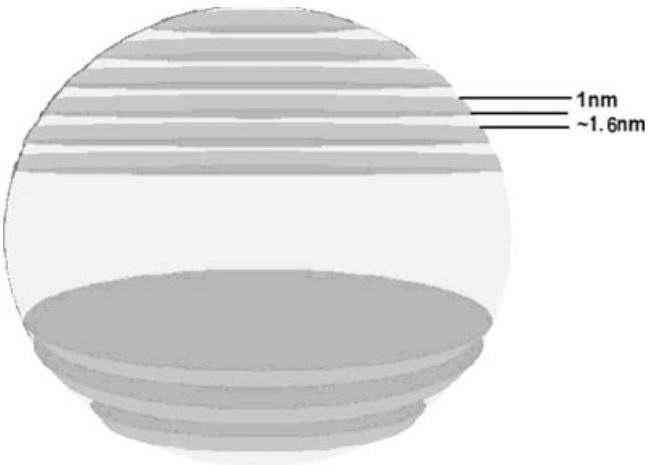

Figure 6 Schematics of a particle consisting of many disk-shaped layers.

$$\langle \cos^2 \phi \rangle = \frac{\int_0^{2\pi} I(\phi)\ \cos^2(\phi)\ \sin(\phi)\ d\phi}{\int_0^{2\pi} I(\phi)\ \sin(\phi)\ d\phi} \tag{3}$$

here I is the intensity of scattering as a function of azimuthal angle β and it can be converted to $I(\phi)$ according to the eq. (4). The angle between the normal to the scattering plane and the shear plane defined by ϕ and θ_B is the Bragg angle.[28]

$$\cos(\beta)\ \cos(\theta_B) = \cos\phi \tag{4}$$

Then the orientation parameter, S_d, was calculated from eq. (5) by using the Herman orientation parameter.[28]

$$S_d = \frac{3\langle \cos(\phi) \rangle - 1}{2} \tag{5}$$

The orientation parameter calculated from experimental data of the partially delaminated 5 wt %I-28/DCPD composite (1-h sonication) cured under shear was ~ 0.1. This is the evidence for the partial orientation of clay platelets and tactoids in the direction of shear. Theoretically, alignment of clay platelets and tactoids perpendicular to the shear direction results in an orientation parameter of -0.5 and full unidirectional alignment in the shear direction will provide an orientation number of 1.

The average as-received I-28 clay particle size is 6–8 μm (range from $\sim$ 1 to16 μm). Assuming these particles are spheres with an average diameter of 7 μm, half of the spherical surface area of one clay particle is 1.54×10^8 nm^2. Subtracting the lateral surfaces of the empty interplatelet space disk shapes, with a thickness of 1.6 nm, the lateral surface area of the platelet disks in a half spherical particle will be 1.06578×10^8 nm^2. Each clay nanolayer has a 2.6 nm d-spacing and consists of a 1-nm thick alumina silicate layer and 1.6-nm thick surfactant (interplatelet) layer (Fig. 6). Therefore, the number of clay nanolayers within a single 7-μm diameter spherical particle is $\sim$ 2700. Each platelet is a thin disk of 1-nm thickness, with a radius that depends on its location in the sphere. The total surface area of all platelets (top and bottom surfaces of these disks + the disks lateral dimensions) for half of the sphere is 6.915×10^{10} nm^2, $\sim$ 650 times larger surface area for one half of the original 7 μm diameter clay particle. A single gram of clay (7 μm diameter) contains 2.65×10^9 particles, using a particle density of 2.1 g/cm^3. This calculation results in a surface area of 355 m^2/g of clay when full exfoliation occurs compared to 0.565 m^2/g for lateral surfaces of the disks in a spherical particle. If monodispersed lateral dimensions are assumed, then the specific surface area will be 600 m^2/g (Fig. 7). The specific surface area determined experimentally was 503 m^2/g for clay I-28, using EGME adsorption. This is rather a good agreement when considering that the clay platelets have irregular shapes and fractal surfaces. Second, the distributions of the disk's lateral dimensions are not as polydisperse as that of disks derived from slicing a sphere into a stack of disks.

The clay surface area increases enormously when the clay is highly delaminated, as indicated by the analysis described earlier. This causes a large viscosity increase in the highly delaminated clay dispersions compared to particulate dispersions. Figures 8(a) and 8(b) and 9 show platelet and tactoid alignments in the direction of shear, which were captured by starting the curing reaction while shearing. Figure 7(a) shows alignment of 5 wt % clay I-28 in DCPD dispersion sonicated for 1 h and cured while shearing. Platelets and tactoids were aligned when 5 wt % clay I-28 dispersion was cured under shear [Fig. 8(b)]. A mixture of large tactoids, small tactoids, and platelets are aligned in the

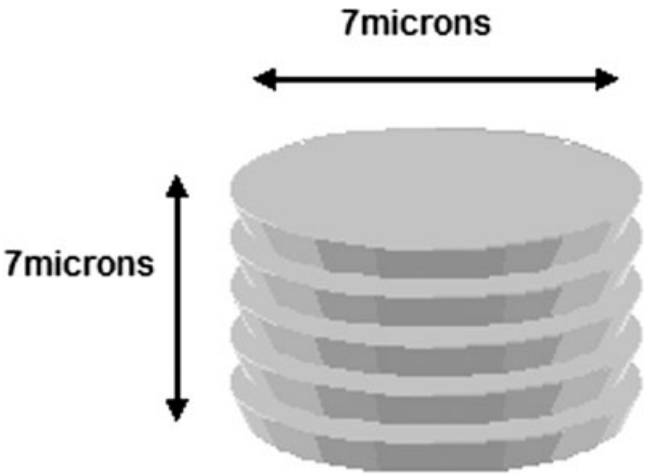

Figure 7 Schematic of monodispersed disk shaped clay platelets.

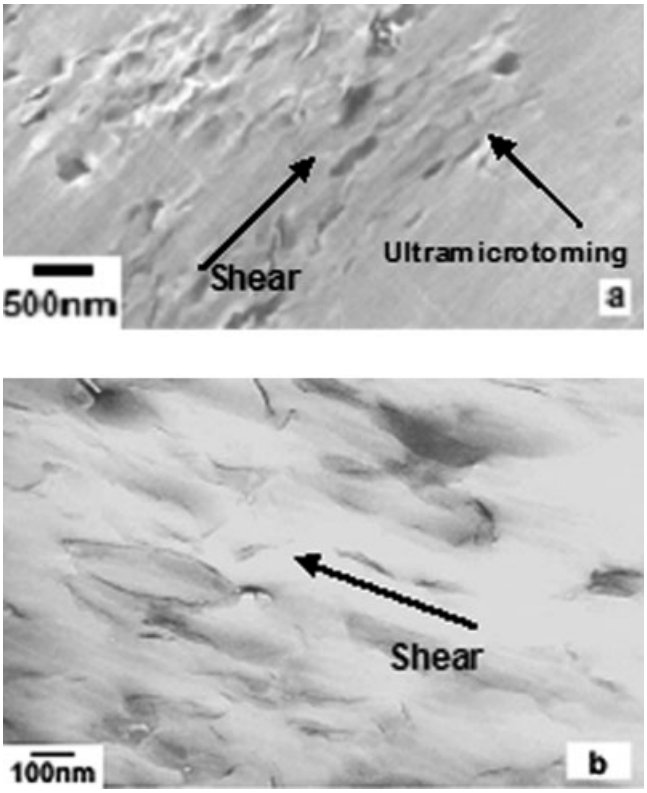

Figure 8 The 5 wt % I-28 clay/DCPD dispersion after polymerizations were conducted in the shear field. Clay platelets and tactoids are partially aligned in the direction of shear. (a) 5 wt % clay I-28/DCPD dispersion at 1 h of sonication (ultramicrotoming direction is perpendicular to the shear direction). (b) 5 wt % I-28 clay dispersion at 3 h of sonication (ultramicrotoming direction is arbitrary).

direction of shear field. Figure 9 demonstrates the alignment of 2 wt % clay I-28, which had been dispersed in DCPD at 3 h of sonication, and then cured while shearing. A high degree of delamination/nanodispersion was present in the sample. Platelets and tactoids are oriented in the shear field. Figure 10 shows the lateral surface of a clay platelet (tactoid) with the lateral dimensions of about 200 $\times$ 350 nm^2. These dimensions were revealed by finding a tactoid that is lying close to a coplanar geometry at the surface.

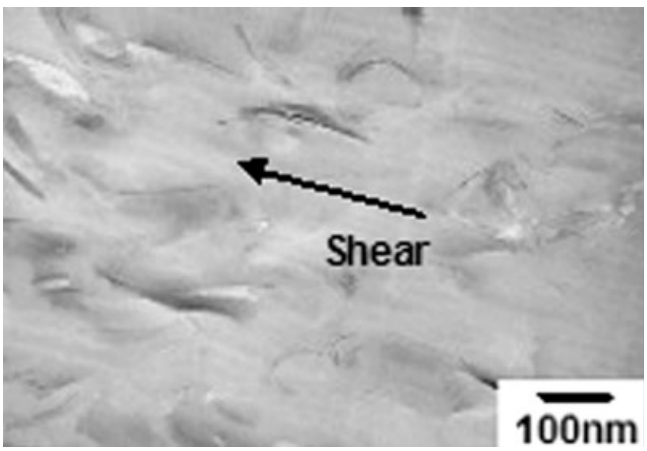

Figure 9 Orientation of tactoids and platelets in the 2 wt % I-28 clay/DCPD dispersion after shearing and curing (ultramicrotoming direction is arbitrary).

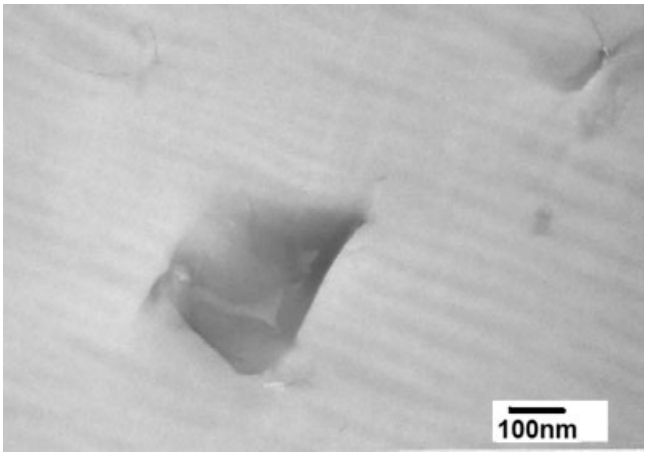

Figure 10 Lateral dimensions of a stack of clay nanolayers.

Oxygen plasma

The surface of the 2 wt % clay I-28 composite was subjected to an oxygen plasma erosion treatment. A low pressure, cold, RF oxygen plasma was employed. Such oxygen plasmas contain O^+, O^-, O_2^+, O, O_3, ionized ozone, metastably excited O_2, and free electrons.[29,30] The electrons, ions, and free radicals in the plasma act on the exposed resin surfaces, generating free radicals at (—CH_2—), (—CH—), and (—CH_3) groups of the hydrocarbon matrix followed by oxidative erosion. The rate of hydrocarbon resin oxidation in the plasma is much faster than the reaction with the alumina silicate platelet sheets. This progressively exposes clay tactoids and platelets at the surface. After 30 s of oxygen plasma exposure, alumina silicate started to protrude from the surface [Fig. 11(a)]. This nanosized alumina silicate platelets protruding from the plasma-eroded composite surface are called nanowalls. After 60-s exposures to the plasma, nanowalls[31] appear that are rising out of surface [Fig. 11(b)]. In Figures 11(a) and 11(b), the spacings between the platelets and tactoids were determined to be in the range of 100–937 nm. Figure 11(b) shows a random tactoid orientation of platelets and tactoids. This sample was not cured under shear or any external force field condition. Lateral dimension of platelets and tactoids were determined to be in the range of $\sim$ 200 to 300 nm. The resolution was not high enough to obtain numerical values for the nanowall thicknesses.

EDS was performed to specify the elements present on the surface of the composite (Fig. 12). EDS verified the presence of aluminum, silicon, oxygen,

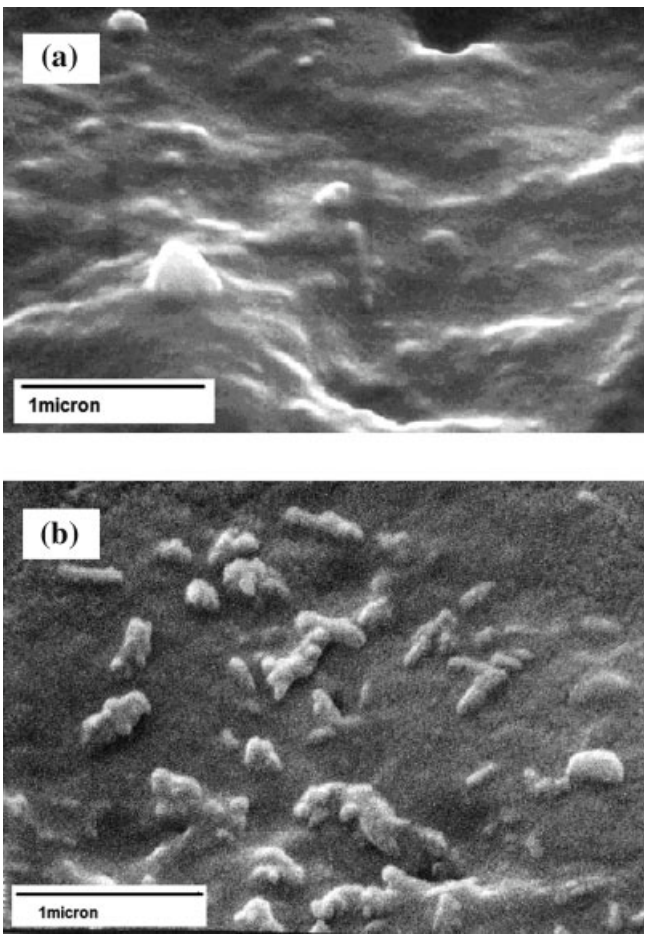

Figure 11 Oxygen plasma-treated surface of the 2 wt % clay I-28/polyDCPD composite. (a) Surface exposed to cold oxygen plasma for 30 s. (b) Surface exposed to cold oxygen plasma for 60 s.

carbon, ruthenium, and chlorine. Chlorine was present in the ruthenium polymerization catalyst. Spectra were taken at different surface locations. Since imaging and EDS were taken at a 45° tilt angle to sample surface, the detector will receive emission of X-rays both from the surface and below the surface. Each spectra revealed some aluminum, silicon, and oxygen, indicating the presence of clay platelets both on the surface and also under the surface. Monte Carlo calculations predict that X-rays are scattered from the surface and beneath the surface up to a depth of about 4–5 μm for a 40 kV voltage.[32] Thus, EDS cannot show specific clay platelet locations.

CONCLUSIONS

XRD and TEM showed that highly delaminated I-28clay/polyDCPD composites were formed by sonicating 6–8-μm sized diameter clay particles in liquid DCPD followed by *in situ* ROMP. Clay loadings ranged from 1 to 5 wt %. Viscosity was related to the degree of delamination. Very low clay concentrations (0.005–0.5 wt %) did not show any time-dependent viscosity behavior. At a 0.5 wt % clay concentration, thixotropic behavior was observed for the nanodispersed clay in DCPD. A Newtonian to non-Newtonian transition occurred at constant clay loading, as the degree of nanodispersion increased during sonication. Thixotropic behavior was observed at concentrations above 0.5–5 wt % I-28 in DCPD, which became more pronounced with increasing clay delamination and higher clay loadings. Viscosity versus shear time is consistent with the align-

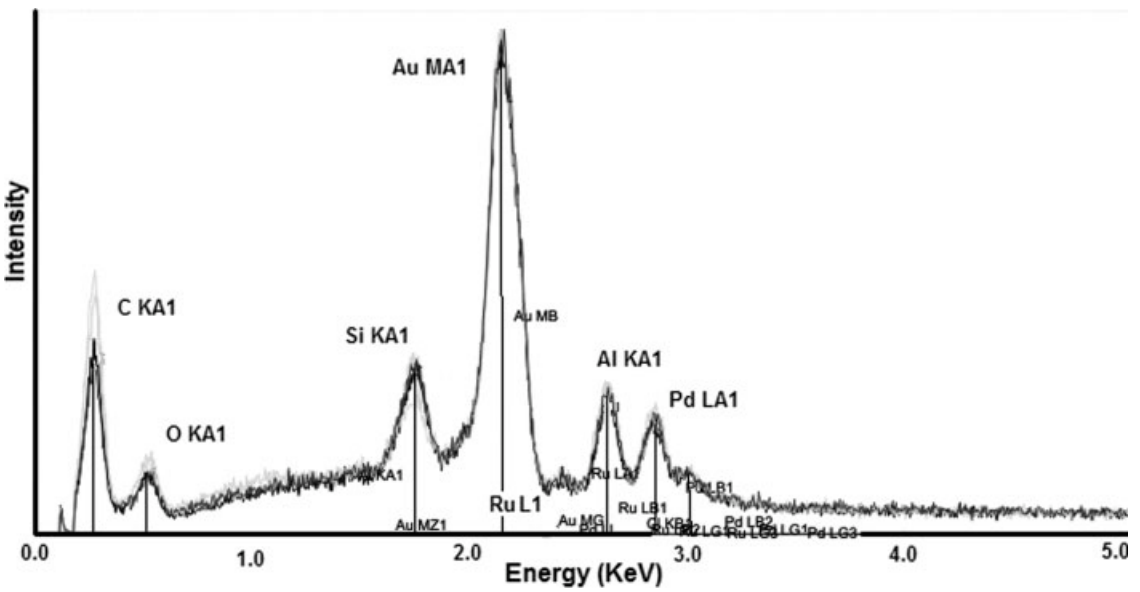

Figure 12 EDS spectra of the oxygen plasma-treated surface of the 2 wt % I-28clay/polyDCPD composite.

ment of tactoids during shear from an original randomly oriented state. This produces a yield stress and a highly thixotropic behavior. Rapid shear thinning suggests that orientation of clay layers occurs in the direction of flow. The viscosity increase is related to the increase in clay tactoid surface area occurring during delamination. TEM studies showed that alignment of the clay layers in the direction of flow could be captured by *in situ* polymerization. The lateral dimensions of some clay platelets (tactoids) lying parallel to the surface were observed. Viscosity measurements could be used as a simple criteria for process control and verification of the degree of delamination. Oxygen plasma treatments of the 2 wt % clay I-28/polyDCPD composite surface led to 3-D observations of protruding clay tactoids.

This method of delaminating clays while suspended in the liquid monomers, followed by shear alignment in the monomer and then by rapid polymerization is a promising method to generate thermoset system containing nanoclay alignment.

The authors acknowledge the award of a Honda Fellowship to M. Yoonessi by the Bagley College of Engineering. The Wright Patterson Air Force Research Laboratories is acknowledged for the use of their X-scattering laboratory. Dr. Hilmar Koerner is thanked for his input on the SAXS data analysis.

References

1. Van Olphen, H. An Introduction to Clay Colloid Chemistry; Wiley: New York, 1997.
2. Mewis, J. J Non-Newtonian Fluid Mech 1979, 6, 1.
3. Luckham, P. F.; Rossi, S. Adv Colloid Interface Sci 1999, 82, 43.
4. Nakaishi, K. Appl Clay Sci 1997, 12, 377.
5. Coussot, P.; Leonov, A. I.; Piau, J. M. J Non-Newtonian Fluid Mech 1993, 46, 179.
6. Barnes, H. A. J Non-Newtonian Fluid Mech 1999, 81, 133.
7. Perret, D.; Locat, J.; Martignoni, P. Eng Geol 1996, 43, 31.
8. Permien, T.; Lagaly, G. Appl Clay Sci 1994, 9, 251.
9. Oka, F. Mech Mater 1993, 16, 47.
10. Lan, T.; Pinnavaia, T. J. Chem Mater 1994, 6, 2216.
11. Brown, J. M.; Curliss, D.; Vaia, R. A. Chem Mater 2000, 12, 3376.
12. Gilman, J. W.; Jackson, C. L.; Morgan, A. B.; Harris, R., Jr.; Manias, E.; Gianneis, E. P.; Wuthenow, M.; Hilton, D. Chem Mater 2000, 12, 1866.
13. Zhu, J.; Wilkie, C. A. Polym Int 2000, 49, 1158.
14. Messersmith, P. B.; Giannelis, E. P. J Polym Sci Part A: Polym Chem 1995, 33, 1047.
15. Chin, I.; Thurn-Albretcht, T.; Kim, H.; Russell, Th. P.; Wang, J. Polymer 2001, 42, 5947.
16. Krishnamarooti, R.; Vaia, R. A.; Giannelis, E. P. Chem Mater 1996, 8, 1728.
17. Morgan, A. B.; Gilman, J. W.; Jackson, C. L. Macromolecules 2001, 34, 2735.
18. Fielding, J. C.; Jacques, Lt. A.SAMPE Proceeding, Long Beach, CA, May 16–22, 2004.
19. Bielawski, C. W.; Grubbs, R. H. Angew Chem Int Ed Engl 2000, 39, 2903.
20. Lynn, D. M.; Kanaoka, S.; Grubbs, R. H. J Am Chem Soc 1996, 118, 784.
21. Maynard, H. D.; Okada, S. Y.; Grubbs, R. H. Macromolecules 2000, 33, 6239.
22. Zhang, D.; Huang, J.; Qian, Y.; Chan, A. S. J Mol Cat A: Chem 1998, 133, 131.
23. Yoonessi, M.; Toghiani, H.; Kingery, W. L.; Pittman, C. U., Jr. Macromolecules 2004, 37, 2511.
24. Yoonessi, M.; Toghiani, H.; Daulton, T. L.; Lin, J. S.; Pittman, C. U., Jr. Macromolecules 2005, 38, 818.
25. Cerato, A. B.; Lutengger, A. J. Geotech Test J 2002, 25, 315.
26. Eirich, F. R., Ed. Rheology Theory and Applications, Vol. 4; Academic Press: New York, 1967.
27. Koerner, H.; Luo, Y.; Li, X.; Cohen, C.; Hedden, R. C.; Ober, C. K. Macromolecules 2003, 36, 1975.
28. DeRouchy, J.; Thurn-Albercht, T.; Russell, T. P.; Kolb, R. Macromolecules 2004, 37, 2538.
29. Kollur, O. S. Application of Plasma Technology for Improved Adhesion of Materials; Pizzi, A., Mittal, K. L., Eds.; Marcel Dekker: New York, NY, 1994; pp 193–204.
30. Swada, Y.; Nakanishi, Y. Compos A 1997, 28: 73.
31. Srtobel, M.; Lyons, C. S.; Mittal, K. L., Eds. Plasma Surface Modification of Polymers: Relevance to Adhesion; VSP: Utrecht, The Netherlands, 1994.
32. Usuki, A.; Hasegawa, N.; Kadoura, H.; Okamoto, T. Nanoletters 2001, 1, 271.